European Radiology (2021) 31:163–170
https://doi.org/10.1007/s00330-020-07081-4

NUCLEAR MEDICINE

Physiologic and hypermetabolic breast 18-F FDG uptake on PET/CT during lactation

Noam Nissan[1,2] · Israel Sandler[1,2] · Michal Eifer[2,3] · Yael Eshet[2,3] · Tima Davidson[2,3] · Hanna Bernstine[2,4] · David Groshar[2,4] · Miri Sklair-Levy[1,2] · Liran Domachevsky[2,3]

Received: 10 June 2020 / Accepted: 16 July 2020 / Published online: 4 August 2020

Abstract

Objective To investigate the patterns of breast cancer-related and lactation-related ^{18}F-FDG uptake in breasts of lactating patients with pregnancy-associated breast cancer (PABC) and without breast cancer.

Methods ^{18}F-FDG-PET/CT datasets of 16 lactating patients with PABC and 16 non-breast cancer lactating patients (controls) were retrospectively evaluated. Uptake was assessed in the tumor and non-affected lactating tissue of the PABC group, and in healthy lactating breasts of the control group, using maximum and mean standardized uptake values (SUVmax and SUVmean, respectively), and breast-SUVmax/liver-SUVmean ratio. Statistical tests were used to evaluate differences and correlations between the groups.

Results Physiological uptake in non-breast cancer lactating patients' breasts was characteristically high regardless of active malignancy status other than breast cancer (SUVmax = 5.0 ± 1.7, $n = 32$ breasts). Uptake correlated highly between the two breasts ($r = 0.61$, $p = 0.01$), but was not correlated with age or lactation duration ($p = 0.24$ and $p = 0.61$, respectively). Among PABC patients, the tumors demonstrated high ^{18}F-FDG uptake (SUVmax = 7.8 ± 7.2, $n = 16$), which was 326–643% higher than the mostly low physiological FDG uptake observed in the non-affected lactating parenchyma of these patients (SUVmax = 2.1 ± 1.1). Overall, ^{18}F-FDG uptake in lactating breasts of PABC patients was significantly decreased by 59% ($p < 0.0001$) compared with that of lactating controls without breast cancer.

Conclusion ^{18}F-FDG uptake in lactating tissue of PABC patients is markedly lower compared with the characteristically high physiological uptake among lactating patients without breast cancer. Consequently, breast tumors visualized by ^{18}F-FDG uptake in PET/CT were comfortably depicted on top of the background ^{18}F-FDG uptake in lactating tissue of PABC patients.

Key Points

- *FDG uptake in the breast is characteristically high among lactating patients regardless of the presence of an active malignancy other than breast cancer.*
- *FDG uptake in non-affected lactating breast tissue is significantly lower among PABC patients compared with that in lactating women who do not have breast cancer.*
- *In pregnancy-associated breast cancer patients, ^{18}F-FDG uptake is markedly increased in the breast tumor compared with uptake in the non-affected lactating tissue, enabling its prompt visualization on PET/CT.*

Keywords Physiological avidity · Benign FDG uptake · Normal FDG uptake · PABC · Breast cancer during lactation

✉ Noam Nissan
noamniss@gmail.com

[1] Department of Radiology, Sheba Medical Center, Emek Ha-Ella 1 st., Tel Hashomer, 5265601 Ramat Gan, Israel

[2] Sackler School of Medicine, Tel Aviv University, Tel Aviv, Israel

[3] Institute of Nuclear Medicine, Sheba Medical Center, Ramat Gan, Israel

[4] Department of Nuclear Medicine, Assuta Medical Centers, Tel Aviv, Israel

Abbreviations

^{18}F-FDG	18 Fluorine fluorodeoxyglucose
BPE	Background parenchymal enhancement
CT	Computed tomography
DCE	Dynamic contrast enhanced
DCIS	Ductal carcinoma in situ
IDC	Invasive ductal carcinoma
MIP	Maximal intensity projection

MRI	Magnetic resonance imaging
PABC	Pregnancy-associated breast cancer
PET	Positron emission tomography
ROI	Region of interest
SUVmax	Maximum standardized uptake value
SUVmean	Mean standardized uptake value

Introduction

During pregnancy and lactation, extensive physiological and morphological modifications take place in the breast, which result in increased size and composition redistribution, notably glandular tissue proliferation in favor of stromal and adipose tissue involution [1]. As the lactating breast is characterized by enriched vascularity, higher parenchymal density, and associated palpable nodularity, its clinical examination and radiological evaluation become challenging [2]. Consequently, the diagnosis of pregnancy-associated breast cancer (PABC), defined as breast cancer diagnosed during pregnancy, lactation or in the first year post-partum, is often delayed, and is therefore associated with an advanced disease at presentation and poor prognosis [3].

Positron emission tomography (PET)/computed tomography (CT) with ^{18}-fluorine fluorodeoxyglucose (^{18}F-FDG) is increasingly being utilized as a management-guiding modality for oncological patients. ^{18}F-FDG-PET/CT has shown to be valuable in staging of locally advanced or metastatic breast cancer [4], with further indications currently under investigation [5–7]. Yet, despite its high sensitivity for detecting malignancies, ^{18}F-FDG uptake in PET/CT could also be attributed to benign conditions [8–10]. Along with other mimickers of breast cancer that can exhibit increased ^{18}F-FDG uptake [11], the lactating breast is a known physiological cause of false-positive uptake, therefore imposing challenges for ^{18}F-FDG-PET/CT interpretation.

Thus far, investigation of physiological lactation-induced ^{18}F-FDG uptake in the breast was limited to a report on seven cases [12] followed by several case reports. Herein, we aimed to elucidate the patterns of breast cancer-related and lactation-related ^{18}F-FDG uptake in breasts of lactating PABC patients and patients without breast cancer.

Materials and methods

This retrospective study was approved by our institutional review board and the requirement for informed consent was waived.

Study population

Cases of patients who underwent radiological evaluations between 2011 and 2020 and were diagnosed with breast cancer during lactation were identified by a computerized search in our institutional radiological information system (RIS). Then, a case-by-case search was performed in the picture archive and communication system (PACS, version 11.0, Carestream Health) to obtain cases that underwent ^{18}F-FDG-PET/CT studies as part of the initial diagnostic workup, as well as breast magnetic resonance imaging (MRI), which served to guide the image analysis. Lactation status at the time of the scan and additional clinical information were obtained from the patients' medical files. In addition, to investigate the characteristics of ^{18}F-FDG uptake in lactating breasts of non-breast cancer patients, an analysis was performed on a matched control group of lactating patients who underwent ^{18}F-FDG-PET/CT for other indications. Controls were retrieved through the RIS as described above.

Acquisition of ^{18}F-FDG-PET/CT

Examinations were performed on two helical CT scanners with 64 or 16 detector rows (Philips Vereos and Philips Gemini GXL, Philips Medical Systems). The field of view and pixel size of the PET images reconstructed for fusion were 57.6 cm and 4 mm, respectively, with a matrix size of 144 × 144. The technical parameters used for CT imaging were pitch, 0.83; gantry rotation speed, 0.5 s/rotation; tube voltage, 120 kVp; modulated tube current, 40–300 mA; and specific breath-holding instructions.

Patients received an intravenous injection of 5.18 MBq/kg ^{18}F-FDG after 4 h of fasting. About 60 min later, CT images were obtained from the vertex to the mid-thigh. If an intravenous contrast material was used, CT scans were obtained 60 s after an injection of 2 ml/kg non-ionic contrast material (Omnipaque 300; GE Healthcare). An emission PET scan followed in a three-dimensional (3D) acquisition mode for the same longitudinal coverage, 1.5 min per bed position. CT images were fused with the PET data, and used to generate a map for attenuation correction, eventually generating reconstructed images for review on a computer workstation (Extended Brilliance Workstation, Philips Medical Systems).

Image analysis

Each ^{18}F-FDG-PET/CT study was separately read by a radiologist with 9 years of experience in breast imaging, and a physician with dual certification in radiology and nuclear medicine with 7 and 12 years of experience in radiology and ^{18}F-FDG-PET/CT reading, respectively. The findings of the reviewers were compared, and discrepancies agreed upon by consensus. The maximum and mean standardized uptake

values (SUVmax and SUVmean, respectively) of ^{18}F-FDG uptake were measured as well as the breast-SUVmax/liver-SUVmean ratio. The latter takes into account the mean liver uptake (measured in the right lobe, omitting significant vessels) as a robust metabolic reference for each exam [13]. This formula may improve tumor characterization [14] while maintaining high reproducibility [15], and reduces differences that are caused by the use of different PET/CT scanners.

For the PABC cohort, spherical regions of interest (ROIs) using a threshold segmentation tool (with 40% threshold) were manually generated in the breast cancer tumor and in the non-affected ipsilateral and contralateral lactating breast tissues. ROIs were carefully delineated using corresponding MRI examinations that indicated the affected and non-affected areas. If the disease was multifocal, ROI was delineated in the largest lesion. In the control cohort, SUV parameters were measured in the entire parenchymal tissue of each breast separately. In addition, a semi-qualitative analysis was performed by dividing ^{18}F-FDG uptake intensity into three subcategories, classifying SUVmax as negligible-low (< 2.5), moderate (2.5–3.5), and high (> 3.5), relative to the normal range of the physiological uptake in the liver, as previously described [8].

Statistical analysis

The normality of the distribution of the ^{18}F-FDG uptake parameters was tested using the Shapiro-Wilk test. Paired two-tailed Student's *t* tests were applied for evaluating intra-individual differences in ^{18}F-FDG parameters of the two breasts, or for comparing breast cancer with the normal ipsi- and contralateral breast tissues. Unpaired two-tailed Student's *t* tests were applied for evaluating differences in ^{18}F-FDG parameters of normal breast parenchyma among breast cancer and non-breast cancer controls. Pearson's tests (Excel 2010, Microsoft) were applied for measuring the correlation between ^{18}F-FDG uptake and age, lactation duration, and the symmetry in uptake between the two breasts. Spearman's test was used for comparing the distribution of categorized qualitative SUV uptake between the PABC and control groups. Statistical significance was defined as $p < 0.05$.

Results

Overall, 16 breast cancer patients (median age, 34 years; range, 25–41) diagnosed during lactation (median lactation duration at the time of examination, 8 months; range, 2–18 months) with initial staging by ^{18}F-FDG-PET/CT comprised the prime study cohort. All PABC lesions (median lesion size, 29 mm; range, 10–80 mm) were intermediate- or high-grade invasive ductal carcinoma (IDC), except for one high-grade ductal carcinoma in situ (DCIS). Patient characteristics are summarized in Table 1.

The control group (median age, 34.5 years; range, 24–44) comprised 16 lactating patients (median lactation duration at the time of examination, 5 months; range, 1–18 months), with ^{18}F-FDG-PET/CT performed for the evaluation of lymphoma ($n = 12$ patients), Castleman disease and malignancy of the lung, thyroid, and endometrium ($n = 1$ patient each).

Table 1 Demographic, clinical, imaging, and pathology characteristics of the PABC cohort. The characteristics of 16 PABC patients are summarized, including age (years) breastfeeding duration (months), presenting symptoms, BRCA status (B), the tumor's maximal diameter per MRI (T), nodal (N), and metastatic involvement (M) as well as pathological results

Subject	Age	Duration	Presentation	B	T	N	M	Pathology
1	31	15	Palpable mass		55	+	+	IDC grade III (ER+, PR−, HER2+)
2	37	16	Palpable mass		16	+	–	IDC grade III (ER+, PR−, HER2−)
3	37	3	Palpable mass	1	12	–	–	IDC grade III (triple negative)
4	31	2	Palpable mass		28	–	–	IDC grade III (ER+, PR−, HER2+)
5	34	8	Palpable mass		16	–	–	IDC grade II (ER+, PR+, HER2−)
6	38	2	Palpable mass		10	+	–	IDC grade III (triple negative)
7	25	8	Palpable mass		67	+	–	IDC grade III (triple negative)
8	31	6	Palpable mass		28	–	–	IDC grade III (ER+, PR+, HER2+)
9	30	14	Palpable mass	2	80	+	–	IDC grade III (triple negative)
10	37	11	Palpable mass		25	+	–	IDC grade III (ER+, PR+, HER−)
11	33	3	Palpable mass		42	–	–	DCIS high-grade (triple negative)
12	41	4	Palpable mass		50	–	–	IDC grade III (ER+, PR+, HER2−)
13	33	4	Palpable mass	1	40	–	–	IDC grade III (triple negative)
14	34	11	Milk rejection	2	30	+	–	IDC grade II (ER+, PR+, HER2+)
15	40	18	Palpable mass		37	+	–	IDC grade III (triple negative)
16	30	11	Milk rejection		11	+	–	IDC grade III (triple negative)

ER estrogen receptor, *PR* progesterone receptor, *HER2* human epidermal growth factor receptor 2

Physiological ^{18}F-FDG uptake in the lactating breast

Physiological uptake in 92% (29/32) of lactating patients' breasts without breast cancer was characteristically high (SUVmax > 3.5). Two exceptions were noted: one patient had an asymmetric uptake exhibiting low uptake in one breast, and one patient showed intermediate and low uptake values in the breasts.

Average breast SUVmax, breast SUVmean, and breast-SUVmax/liver-SUVmean ratio values were 5.0 ± 1.7, 2.7 ± 1.1, and 2.7 ± 0.6, respectively ($n = 32$ breasts). Both SUVmax and SUVmean were highly correlated between the right and left breasts of each patient ($r = 0.61$, $p = 0.01$, and $r = 0.58$, $p = 0.02$, respectively). Comparable ^{18}F-FDG uptake values ($p = 0.77$) were found in the breasts of patients who had active disease during the scan ($n = 6$, SUVmax = 5.6 ± 2.1) and patients who were on follow-up with no evidence of active disease ($n = 10$, SUVmax = 5.7 ± 1.5). Variations in uptake parameters were more apparent among patients (average inter-individual CV = 34%) than between the right and left breasts of each individual patient (average intra-individual CV = 17%). Uptake values were not correlated with age or lactation duration ($p = 0.24$ and $p = 0.61$, respectively).

Representative images of ^{18}F-FDG-PET/CT exams of a lactating lymphoma patient are shown in Fig. 1, highlighting the high, but not symmetrical, physiological uptake in the two breasts that diminished completely in the follow-up scan upon breastfeeding weaning.

Hypermetabolic and physiological ^{18}F-FDG uptake in PABC patients' breasts

All PABC tumors ($n = 16$) were readily visible on top of the background lactation-related parenchymal ^{18}F-FDG uptake. Most lesions (12/16, 75%) exhibited high ^{18}F-FDG uptake, while the remaining lesions demonstrated intermediate and low uptake (2/16, 12.5% for each category). The average breast cancer lesion SUVmax, SUVmean, and breast tumor-SUVmax/liver-SUVmean ratio were 7.8 ± 7.2, 4.6 ± 3.9, and 4.4 ± 4.5, respectively. Representative images of lactating PABC patients (Figs. 2 and 3) highlight the marked hypermetabolic uptake of the PABC tumors relative to the reduced uptake in the surrounding non-affected parenchyma. Physiological ^{18}F-FDG uptake in the non-affected parenchyma of PABC patients was low in most patients (25/32 breasts, 78%). Four patients demonstrated different right and left breast ^{18}F-FDG uptake (high and high, high and moderate, high and low, moderate and moderate). The average breastSUVmax, breastSUVmean, and breast-SUVmax/

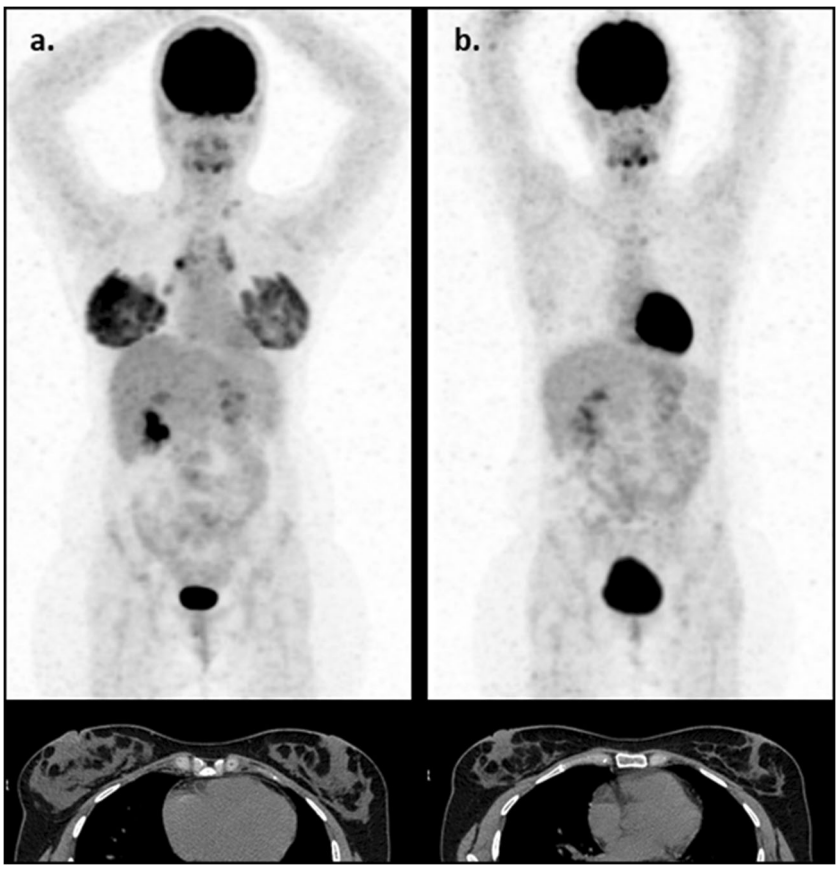

Fig. 1 Sequential ^{18}F-FDG-PET/CT images during lactation and post-weaning. Whole body maximal intensity projection (MIP) PET and axial non-contrast CT images at the height of the mid breast of a 27-year-old patient monitored for lymphoma. (**a**) Images acquired during lactation, which lasted 4 months, show high physiological uptake of ^{18}F-FDG in the breasts. Note that uptake was higher in the right compared with the left breast (SUVmax = 8.4 vs. 6.2). (**b**) Images acquired post-weaning, 63 days after the images shown in (**a**), show that physiological uptake diminished completely. The CT images demonstrate the marked reduction in breast density and increase in fatty tissue post-weaning

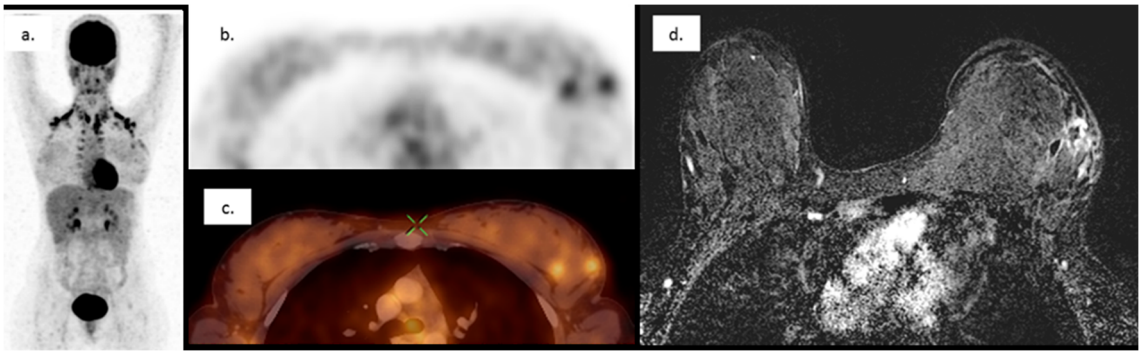

Fig. 2 Representative ^{18}F-FDG-PET/CT images of PABC patient breasts. Images of whole-body MIP ^{18}F-FDG-PET (**a**), axial ^{18}F-FDG-PET (**b**), axial-fused PET/CT **(c)**, at the height of two PABC tumors and their corresponding subtraction-DCE-MRI (**d**) of a 33-year-old patient with newly diagnosed multifocal triple-negative high-grade IDC. The patient, a BRCA1 carrier, was diagnosed while lactating for 4 months. The high hypermetabolic ^{18}F-FDG uptake of the two tumor foci (SUVmax = 4.1) showed intermediate to high uptake compared with the non-negligible physiological uptake of the non-affected parenchyma (SUVmax = 2.8 for both breasts), allowing cancer detection. The adjunct MR images highlight the prominent typical BPE of lactation, which, like ^{18}F-FDG uptake on PET/CT, does not prohibit tumor visibility with greater contrast enhancement

liver-SUVmean ratio of the normal lactating breast tissue among the PABC patients were 2.1 ± 1.1, 1.1 ± 0.6, and 1.1 ± 0.5 ($n = 32$ breasts), respectively. In each patient, the ipsi- and contralateral normal lactating breast tissues showed similar ^{18}F-FDG SUVmax and SUVmean values ($p = 0.16$ and $p = 0.37$, respectively, for the difference in uptake between breasts). SUVmax and SUVmean values were also highly correlated between the right and left breasts of each patient ($r = 0.69$, $p < 0.005$; and $r = 0.70$, $p < 0.005$, respectively). Variations in uptake parameters were more apparent among patients (average inter-individual CV = 52–53%) than between the breasts of each individual patient (average intra-individual CV = 13%). Comparison between tumor SUVmax and physiological breast SUVmax and breast SUVmean in PABC patients showed that, on average, the tumors demonstrated 326% and 643% more avidity, respectively, stressing the marked parametric contrast of the tumors on top of the normal lactating tissue background.

Comparison between PABC and control groups

Comparison between the physiological uptake of ^{18}F-FDG in PABC patients and controls showed that lactation-induced uptake in lactating breasts of PABC patients was significantly lower by 59% compared with that of lactating controls without breast cancer ($p < 0.0001$). On average ^{18}F-FDG uptake among lactating controls without breast cancer represented 241–246% of the uptake among PABC patients. Summary of the results and illustration of the of measurements' distribution between the groups of PABC and non-breast cancer lactating controls are presented by box-and-whisker analysis in Fig. 4.

Discussion

Imaging of the lactating breast provides a view of the dramatic anatomical changes that take place within this dynamic organ once it reaches its ultimate functional competency. Identifying

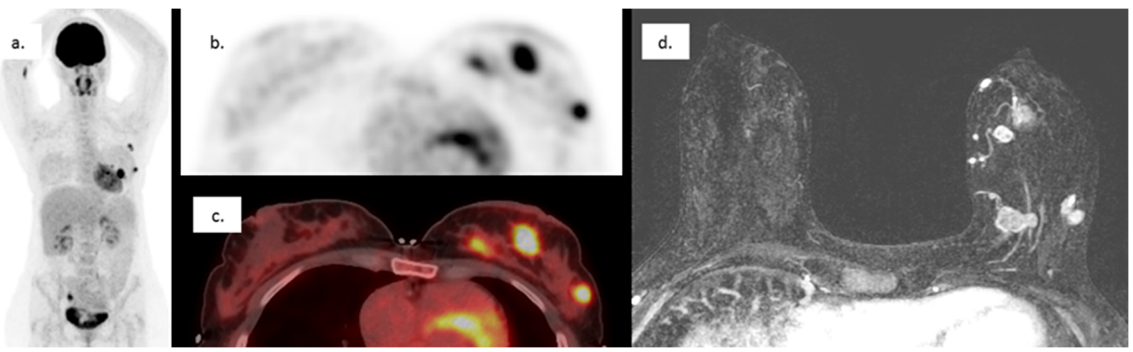

Fig. 3 Representative ^{18}F-FDG-PET/CT images of PABC patient breasts. Images of whole body MIP ^{18}F-FDG-PET (**a**), axial ^{18}F-FDG-PET (**b**), axial-fused PET/CT (**c**), at the height of three PABC tumors and their corresponding subtraction-DCE-MRI (**d**) of a 40-year-old patient who had been lactating for 18 months when diagnosed with multifocal triple-negative high-grade IDC. High hypermetabolic ^{18}F-FDG uptake was demonstrated by the tumor foci (SUVmax = 8.1), on top of a low, but noticeable, physiological uptake in the non-affected parenchyma (SUVmax = 2.0 and 1.8 for the ipsi- and contralateral breast, respectively)

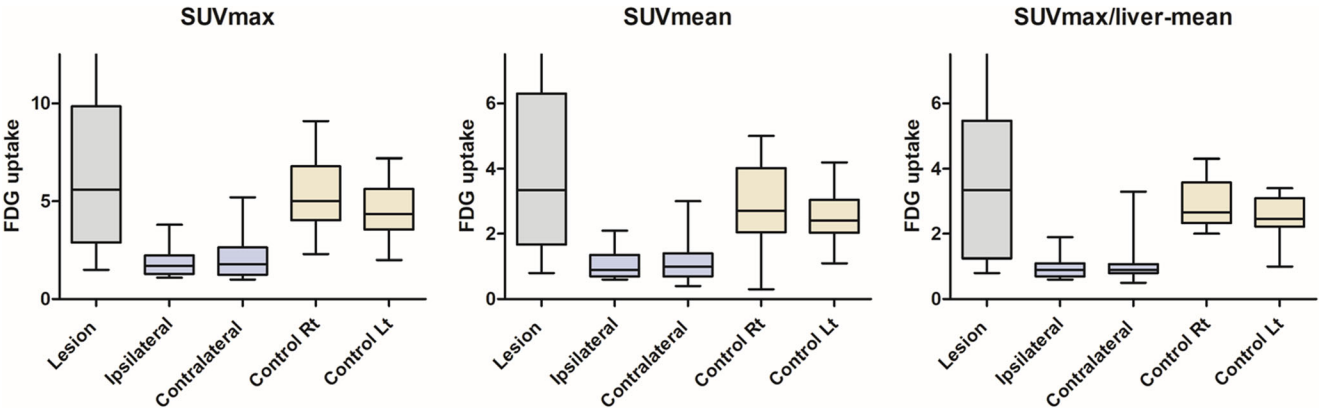

Fig. 4 ^{18}F-FDG uptake in lactating PABC patients compared with lactating women without breast cancer (control). Box plots showing the median ± interquartile range (IQR) and whiskers (± 1.5 IQR) of the ^{18}F-FDG uptake parameters (SUVmax, SUVmean, and SUVmax/SUV liver mean) measured in PABC lesions, in the ipsi- and contralateral surrounding lactating tissue of the PABC patients, and in the healthy right and left lactating breasts of the control group (n = 16). The plots highlight the statistically significant increased uptake in the PABC lesion and the controls, compared with the uptake in healthy lactating tissue of the PABC group, regardless of the measured parameter

the unique imaging characteristics of breast tissue with a normal structure and function is clinically important for differentiating between lactation-related modifications and pathologies, particularly, PABC. In recent years, dynamic contrast-enhanced (DCE) MRI studies enabled to visualize and quantify the increased fraction of fibroglandular tissue [16], and the increased vascular supply of the lactating breast [17]. Further clinical DCE MRI studies reported on the marked background parenchymal enhancement (BPE) of the lactating breast [18, 19], which causes decreased tumor conspicuity [20]. Additional characterization of the structural changes that take place in lactating breasts was afforded by unenhanced diffusion MRI studies, which reported reduced breast diffusivity [21], reduced anisotropy [22, 23], and increased pseudo-diffusion [24], as a result of increased milk viscosity, the underlying microstructural changes and increased perfusion fraction, respectively. Longitudinal studies confirmed the eventual regression of these changes upon involution post-weaning [16, 24]. More recently, preliminary clinical studies among PABC cohorts showed promising results for unenhanced MRI techniques in diagnosis [20, 25] and staging [26, 27].

The increased mammary vasculature serves to supply the increased metabolic activity imposed by lactation [28]. Throughout the course of lactogenesis (milk synthesis and secretion), the mammary vascular network expanses and accompanied together with cellular endothelium transformation, including increase in the cellular surface size and profound increase in the number of mitochondria, that indicate the high imposed metabolic demand [29]. As ^{18}F-FDG-PET provides a sensitive means of metabolic imaging [30], it is particularly suitable for characterizing the high metabolic activity of lactating breasts.

In this study, we investigated the patterns of both physiological and breast tumor (hypermetabolic) ^{18}F-FDG uptake in lactating breasts. Our results emphasize the high bilateral physiological ^{18}F-FDG uptake among the majority of lactating breasts without breast cancer, and are in agreement with past reports [12, 31]. Bakheet and Hammami classified iodine isotope uptake in lactating breasts as four qualitative patterns: full, focal, crescent, and irregular, with "full" being the most common [32]. Our quantitative analyses suggest that lactating breast ^{18}F-FDG uptake might be more complex than is apparent, because the consistent differences noted between SUVmax and SUVmean imply heterogenous intra-individual uptake even in patients with seemingly complete uptake. Furthermore, based on the significant CV between subjects and between the two breasts, together with the lack of correlation between uptake values and age or lactation duration, we propose that uptake values and patterns are likely to be dynamic. Other factors, including technical ones, such as the time between ^{18}F-FDG injection and the PET scan, and behavioral factors, such as breastfeeding patterns (e.g., amount, frequency, dominant breast), and the timing of last nursing before the PET/CT study, which were not documented in our patient files, could all potentially affect uptake measurements and its eventual pattern, thus preventing clear-cut classification of the uptake patterns.

Nevertheless, several distinct findings were observed in our study, mainly in distinguishing between uptake patterns of lactating PABC patients and lactating women that did not have breast cancer. First, among PABC patients, the tumor's hypermetabolic uptake systematically obtrudes, by a comfortable margin, upon the background physiological uptake of the non-affected (both ipsi- and contralateral) lactating parenchyma, enabling the straightforward visualization of all PABC lesions. Thus, the physiological ^{18}F-FDG uptake values of the normal lactating breast parenchyma of PABC patients were markedly decreased in comparison with physiological ^{18}F-FDG uptake values measured in the control group, including those patients who had an active malignant disease other

than breast cancer. This finding highlights the prominent local energetic burden of breast cancer, in contrast with the general metabolic demand of other malignancies that do not directly compete with the local physiological metabolic demands of lactation. Related observations on the effect of breast tumors on healthy breast parenchyma were recently described by Leithner and colleagues, who reported that the ^{18}F-FDG-PET/MRI biomarkers BPE and breast parenchymal uptake were significantly decreased in the contralateral tumor-free breast tissue of patients with malignant breast tumors compared with that of patients with benign breast lesions [33].

From a clinical standpoint, this work supports the utilization of ^{18}F-FDG-PET/CT during lactation, without the need to postpone the exam, such as in the case of breast MRI [34]. Our results show that breast cancers are easily depicted, preserving the capabilities of ^{18}F-FDG-PET/CT in loco-regional staging and as a prognostic tool among PABC patients [4]. Furthermore, although infrequent, metastatic disease in the breast [35] or an incidental second primary breast lesion [36] could be potentially detected among non-breast cancer lactating patients undergoing ^{18}F-FDG-PET/CT.

Several limitations of this study should be noted. Firstly, due to the rarity of the disease, the PABC cohort was relatively small, restricting further subgroup analyses. Moreover, the control group was assembled based on the retrospective identification of the lactating state in the radiological reports; therefore, a potential selection bias may have been introduced to the study due to the inclusion of examinees for whom a high physiological uptake was noted in the report and the potential omission of lactating patients with a low uptake that was not reported, and hence missed by our search. Finally, due to the retrospective nature of the study, the groups were not standardized, consequently limiting the efficacy of the applied correlation tests in the absence of in-depth information about the breastfeeding habits at the time of the scan.

In conclusion, high physiological ^{18}F-FDG uptake in lactating breasts is demonstrated on PET/CT with variable quantities among examinees. Despite the high congruence of uptake in the two breasts of individual patients, asymmetrical uptake might be encountered. Among PABC patients undergoing ^{18}F-FDG-PET/CT, the tumor's hypermetabolic ^{18}F-FDG uptake is significantly higher than the physiological uptake of the surrounding non-affected lactating fibroglandular tissue, which in turn, is much lower than the uptake noted for non-breast cancer lactating breasts.

Funding information The authors state that this work has not received any funding.

Compliance with ethical standards

Guarantor The scientific guarantor of this publication is Dr. Noam Nissan.

Conflict of interest The authors of this manuscript declare no relationships with any companies, whose products or services may be related to the subject matter of the article.

Statistics and biometry One of the authors has significant statistical expertise.

Informed consent Written informed consent was waived by the Institutional Review Board.

Ethical approval Institutional Review Board approval was obtained.

Methodology
- retrospective
- case-control study
- performed at one institution

References

1. McManaman JL, Neville MC (2003) Mammary physiology and milk secretion. Adv Drug Deliv Rev 55:629–641
2. Vashi R, Hooley R, Butler R, Geisel J, Philpotts L (2013) Breast imaging of the pregnant and lactating patient: physiologic changes and common benign entities. AJR Am J Roentgenol 200:329–336. https://doi.org/10.2214/AJR.12.9845
3. Langer A, Mohallem M, Stevens D, Rouzier R, Lerebours F, Chérel P (2014) A single-institution study of 117 pregnancy-associated breast cancers (pabc): presentation, imaging, clinicopathological data and outcome. Diagn Interv Imaging 95:435–441. https://doi.org/10.1016/j.diii.2013.12.021
4. Rosen EL, Eubank WB, Mankoff DA (2007) FDG PET, PET/CT, and breast cancer imaging. Radiographics 27 Suppl 1:S215-S229
5. Graña-López L, Herranz M, Domínguez-Prado I, Argibay S, Villares A, Vázquez-Caruncho M (2020) Can dedicated breast PET help to reduce overdiagnosis and overtreatment by differentiating between indolent and potentially aggressive ductal carcinoma in situ? Eur Radiol 30(1):514–522
6. Bakhshayeshkaram M, Salehi Y, Abbasi M et al (2019) A preliminary study to propose a diagnostic algorithm for PET/CT-detected incidental breast lesions: application of BI-RADS lexicon for US in combination with SUVmax. Eur Radiol 29(10):5507–5516
7. Botsikas D, Bagetakos I, Picarra M et al (2019) What is the diagnostic performance of 18-FDG-PET/MR compared to PET/CT for the N- and M- staging of breast cancer? Eur Radiol 29(4):1787–1798
8. Davidson T, Lotan E, Klang E et al (2018) Fat necrosis after abdominal surgery: a pitfall in interpretation of fdg-pet/ct. Eur Radiol 28:2264–2272. https://doi.org/10.1007/s00330-017-5201-5
9. Lobert P, Brown RKJ, Dvorak RA, Corbett JR, Kazerooni EA, Wong KK (2013) Spectrum of physiological and pathological cardiac and pericardial uptake of FDG in oncology PET-CT. Clin Radiol 68:e59–e71. https://doi.org/10.1016/j.crad.2012.09.007
10. Nishizawa S, Inubushi M, Okada H (2005) Physiological 18F-FDG uptake in the ovaries and uterus of healthy female volunteers. Eur J Nucl Med Mol Imaging 32:549–556. https://doi.org/10.1007/s00259-004-1703-x
11. Adejolu M, Huo L, Rohren E, Santiago L, Yang WT (2012) False-positive lesions mimicking breast cancer on FDG PET and PET/CT. AJR Am J Roentgenol 198:304–314. https://doi.org/10.2214/AJR.11.7130
12. Hicks RJ, Binns D, Stabin MG (2001) Pattern of uptake and excretion of 18F-FDG in the lactating breast. J Nucl Med 42:1238–1242

13. Domachevsky L, Bernstine H, Nidam M et al (2017) Hepatic 18F-FDG uptake measurements on PET/MR: impact of volume of interest location on repeatability. Contrast Media Mol Imaging. https://doi.org/10.1155/2017/8639731
14. Park J, Chang KJ, Seo YS et al (2014) Tumor SUVmax normalized to liver uptake on 18F-FDG PET/CT predicts the pathologic complete response after neoadjuvant chemoradiotherapy in locally advanced rectal cancer. Nucl Med Mol Imaging 2010. https://doi.org/10.1007/s13139-014-0289-x
15. Viner M, Mercier G, Hao F, Malladi A, Subramaniam RM (2013) Liver SULmean at FDG PET/CT: interreader agreement and impact of placement of volume of interest. Radiology. https://doi.org/10.1148/radiol.12121385
16. Nissan N, Furman-Haran E, Shapiro-Feinberg M, Grobgeld D, Degani H (2017) Monitoring in-vivo the mammary gland microstructure during morphogenesis from lactation to post-weaning using diffusion tensor MRI. J Mammary Gland Biol Neoplasia 22(3):193–202
17. Espinosa LA, Daniel BL, Vidarsson L, Zakhour M, Ikeda DM, Herfkens RJ (2005) The lactating breast: contrast-enhanced MR imaging of normal tissue and cancer. Radiology 237:429–436. https://doi.org/10.1148/radiol.2372040837
18. Taron J, Fleischer S, Preibsch H, Nikolaou K, Gruber I, Bahrs S (2018) Background parenchymal enhancement in pregnancy-associated breast cancer: a hindrance to diagnosis? Eur Radiol 29(3):1187-1193
19. Myers KS, Green LA, Lebron L, Morris EA (2017) Imaging appearance and clinical impact of preoperative breast MRI in pregnancy-associated breast cancer. AJR Am J Roentgenol W1–W7. https://doi.org/10.2214/AJR.16.17124
20. Nissan N, Allweis T, Menes T et al (2019) Breast MRI during lactation: effects on tumor conspicuity using dynamic contrast-enhanced (DCE) in comparison with diffusion tensor imaging (DTI) parametric maps. Eur Radiol 30(2):767–777
21. Sah RG, Agarwal K, Sharma U, Parshad R, Seenu V, Jagannathan NR (2015) Characterization of malignant breast tissue of breast cancer patients and the normal breast tissue of healthy lactating women volunteers using diffusion MRI and in vivo 1H MR spectroscopy. J Magn Reson Imaging 41:169–174. https://doi.org/10.1002/jmri.24507
22. Nissan N, Furman-Haran E, Shapiro-feinberg M (2014) Diffusion-tensor MR imaging of the breast: hormonal regulation. Radiology 271:672–680
23. Nissan N, Furman-Haran E, Feinberg-Shapiro M et al (2014) Tracking the mammary architectural features and detecting breast cancer with magnetic resonance diffusion tensor imaging. J Vis Exp 1–18. https://doi.org/10.3791/52048
24. Iima M, Kataoka M, Sakaguchi R et al (2018) Intravoxel incoherent motion (IVIM) and non-Gaussian diffusion MRI of the lactating breast. Eur J Radiol Open 5:24–30. https://doi.org/10.1016/j.ejro.2018.01.003
25. Nissan N, Furman-Haran E, Allweis T et al (2018) Noncontrast breast MRI during pregnancy using diffusion tensor imaging: a feasibility study. J Magn Reson Imaging:1–10. https://doi.org/10.1002/jmri.26228
26. Peccatori FA, Codacci-Pisanelli G, Del Grande M, Scarfone G, Zugni F, Petralia G (2017) Whole body MRI for systemic staging of breast cancer in pregnant women. Breast. https://doi.org/10.1016/j.breast.2017.07.014
27. Kosmin M, Makris A, Joshi PV, Ah-See ML, Woolf D, Padhani AR (2017) The addition of whole-body magnetic resonance imaging to body computerised tomography alters treatment decisions in patients with metastatic breast cancer. Eur J Cancer 77:109–116. https://doi.org/10.1016/j.ejca.2017.03.001
28. Butte NF, King JC (2005) Energy requirements during pregnancy and lactation. Public Health Nutr. https://doi.org/10.1079/phn2005793
29. Djonov V, Andres AC, Ziemiecki A (2001) Vascular remodelling during the normal and malignant life cycle of the mammary gland. Microsc Res Tech 15;52(2):182–189
30. Kudo T (2007) Metabolic imaging using PET. Eur J Nucl Med Mol Imaging 34. https://doi.org/10.1007/s00259-007-0440-3
31. Yasuda S, Fujii H, Takahashi W, Takagi S, Ide M, Shohtsu A (1998) Lactating breast exhibiting high F-18 FDG uptake. Clin Nucl Med. https://doi.org/10.1097/00003072-199811000-00010
32. Bakheet SM, Hammami MM (1994) Patterns of radioiodine uptake by the lactating breast. Eur J Nucl Med. https://doi.org/10.1007/BF00285581
33. Leithner D, Helbich TH, Bernard-Davila B et al (2020) Multiparametric 18F-FDG PET/MRI of the breast: are there differences in imaging biomarkers of contralateral healthy tissue between patients with and without breast cancer? J Nucl Med 61:20–25. https://doi.org/10.2967/jnumed.119.230003
34. diFlorio-Alexander RM, Slanetz PJ, Moy L et al (2018) ACR Appropriateness Criteria® breast imaging of pregnant and lactating women. J Am Coll Radiol. https://doi.org/10.1016/j.jacr.2018.09.013
35. Benveniste AP, Marom EM, Benveniste MF, Mawlawi OR, Miranda RN, Yang W (2014) Metastases to the breast from extramammary malignancies - PET/CT findings. Eur J Radiol 83(7):1106–1112.
36. Benveniste AP, Marom EM, Benveniste MF, Mawlawi O, Fox PS, Yang W (2015) Incidental primary breast cancer detected on PET–CT. Breast Cancer Res Treat 151(2):261–268